JOURNAL OF MATERIALS SCIENCE 20 (1985) 3661–3667

Influence of fibre orientation on acoustic emission from filament wound pipes

IRENEUSZ JERZYK, MACIEJ KUMOSA*
Instutute of Materials Science and Applied Mechanics, Technical University of Wroclaw, Wroclaw, Poland

The effect of the winding angle of filament wound pipes internally pressurized was investigated by means of the acoustic emission technique. The acoustic emission results were correlated with the theoretical data of the state of stress at the matrix–fibre boundary. The experimental results showed that acoustic emission strongly depended on fibre orientation. Acoustic emission signals were mainly caused by two types of failure of the composite: debonding on the matrix–fibre interface and transverse cracks in the lamina. The influence of fibre rotation on the acoustic emission behaviour was also taken into account. It is stated that the significant start of acoustic emission is due to cohesive cracking at the matrix–fibre boundary when the normal stress, $\sigma_{\perp}$ to the fibre overreached the critical value of 11.5 MPa for all considered fibre orientations.

1. Introduction

During the last several years there have been many works directed towards the identification of different types of deformation mechanisms producing acoustic emission (AE) events in glass–fibre reinforced plastics (GRP). The usage of AE as a monitoring system [1–5] has made it possible to detect failure processes occurring during the loading of GRP. The major acoustic emission sources, related to deformation modes that take place within the material, can be classified in the following way [6]: fibre cracking, fibre–matrix interfacial debonding, matrix plastic deformation and cracking, interlaminar debonding and rubbing of the fibre against the matrix. Acoustic emission activity and emission energy are functions of source density and the energy released during formation of AE sources. Since the deformation and fracture behaviour of GRP in reality depends on fibre orientation towards the applied stress, it can be expected that the effect of orientation should also be reflected in the AE activity.

The main aim of the study was to investigate the fibre orientation in pressurized filament wound pipes and to correlate it with the changes in AE activity. Acoustic emission was mainly caused by the following two kinds of failure: cracks at the matrix–fibre interface and transverse cracks in a lamina. For fracture to occur, some form of internal stress concentration is required to raise the local stress level to the critical value.

Assuming the mode of loading is a constant and taking into account various fibre orientations enables us to vary the stress distribution around the fibres. As a result, the differences in the intensity of the deformation mechanisms inside the pipes as well as in acoustic emission activity have been observed.

2. Materials and experimental methods

Fibre-reinforced pipes, in which glass–fibres were wound at angles of 15°, 23°, 32° and 45° using Fibreglass ER 2003 PID constituted the

Present address: Department of Metallurgy and Materials Science, University of Cambridge, Pembroke Street, Cambridge CB2 3QZ, UK.

0022–2461/85 $03.00 + .12

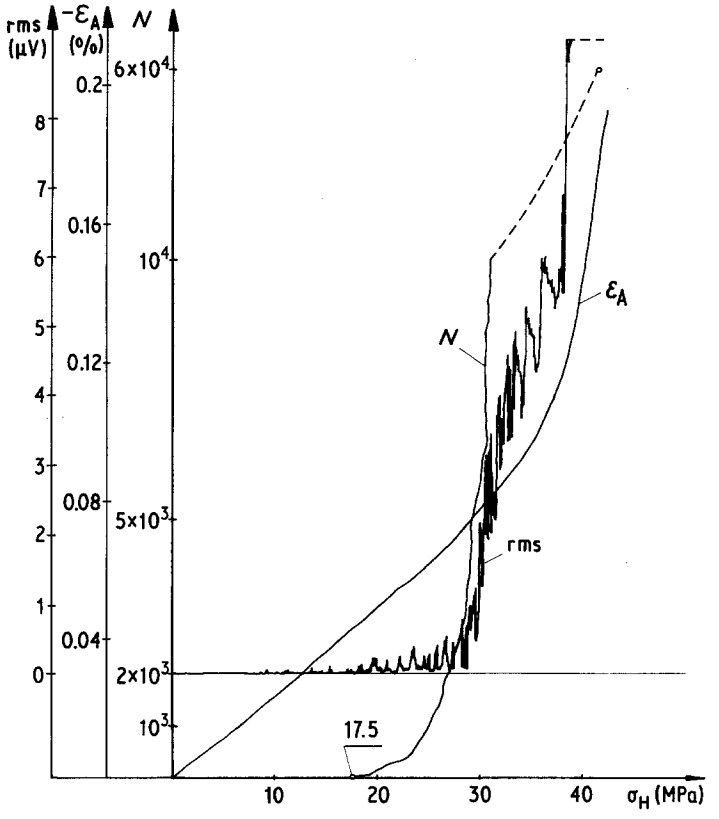

Figure 1 Typical cumulative counts N, rms voltage and axial strain, ε_A, plotted against σ_H for $\Phi = 23°$.

samples used in the investigations. The resin utilized was epoxy resin (Epon 5).

The pipes were made up of twelve complete laminas with a diameter of 25 mm and the thickness equal to 2 mm. The average volume of fibre fraction for all kinds of pipes was $V_f = 44\%$. The length of the pipes was 340 mm. All the pipes were internally pressurized by oil at the rate of $10\,\text{MPa}\,\text{min}^{-1}$. The loading conditions were similar to Mode III in the Hull *et al.* experiments [7]. Both ends of the pipe were free to slide on seals. The hoop stress, σ_H, and the axial strain, ε_A were dependent on the internal pressure and the elastic properties of the pipes; however, the axial stress, σ_A, was always zero.

A signal processor (Model 201, Acoustic Emission Technology Corporation, Sacramento, California) with a sensor of a nominal resonance frequency of 175 kHz and a preamplifier Model 160, AET were used as a monitoring system. The time constant of the rms voltage measurement was 5 msec. All tests were performed with a total gain of 98 dB. The sensor was attached in the middle of the pipe on its external surface.

3. Results

Two types of acoustic emission parameters rms voltage and cumulative counts, N, from the pressurized pipes with various fibre orientation were recorded. The AE data were analysed as a function of the hoop stress, σ_H. The strain, ε_A, in the pipe was measured in the axial direction only by means of a strain gauge.

The results of rms and N as well as ε_A were similar but there were some differences in details in all the considered fibre orientations. Fig. 1 shows typical cumulative counts N, rms and ε_A plotted against σ_H for the pipe with a fibre winding angle $\Phi = 23°$, which was chosen as a representative example of AE behaviour from all the pipes. At low pressure the pipe showed linear elastic properties (ε_A is a linear function of σ_H). In this range of loading, accidental weak AE signals appeared. As the pressure increased systematic AE was observed at $\sigma_H = 17.5$ MPa. In the range of a well defined transition to nonlinear behaviour of ε_A AE activity increased. The fracture of the pipe with $\Phi = 23°$ occurred at the average hoop stress of $\sigma_H = 41.3$ MPa. Actually, no real changes in AE behaviour were

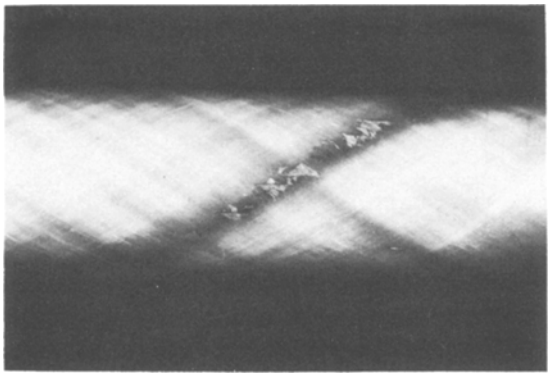

Figure 2 Final failure area of a pipe with $\Phi = 32°$ tested to fracture.

observed within the range of pressure beginning with distinct non-linearity and ending at the moment of fracture. There were no signs of weepage before the fracture.

Fig. 2 presents a photograph of the pipe of $\Phi = 32°$ after fracture which is representative of the appearance of the final failure area of all the pipes. Fracture was associated with a narrow dark band which formed a spiral along the pipe in the fibre direction. At low pressures the stress/strain response of all the tested pipes was linear (Fig. 3).

The axial strains ε_A were always negative in contrast to the hoop stresses which were positive. The slope σ_H/ε_A increased as Φ increased. Also, the onset of non-linearity of ε_A took place at a higher level of σ_H. The strength properties of the pipes increased progressively as Φ increased.

There is a correlation between the axial strain behaviour and the corresponding number of counts, N, as a function of σ_H (Fig. 4). The significant start of AE appeared at a higher σ_H with increasing Φ. AE activity, $\Delta N/\Delta\sigma_H$, and the total number of counts, N_T, at the moment of fracture depended strongly on the fibre orientation and were greatest for small Φ.

The most important mechancial properties and corresponding AE data of all the tested pipes are summarized in Table I. All the results should be treated as average values attributed to at least three tests for each winding angle. There was a reasonable scatter of results of the hoop stress, σ_H, at the moment of noticeable start of AE for all tested winding angles, see Fig. 5.

4. Discussion

According to Hull *et al.* [7] the first microcracks in filament wound glass-fibre polyester pipes occur as a result of the debonding of individual

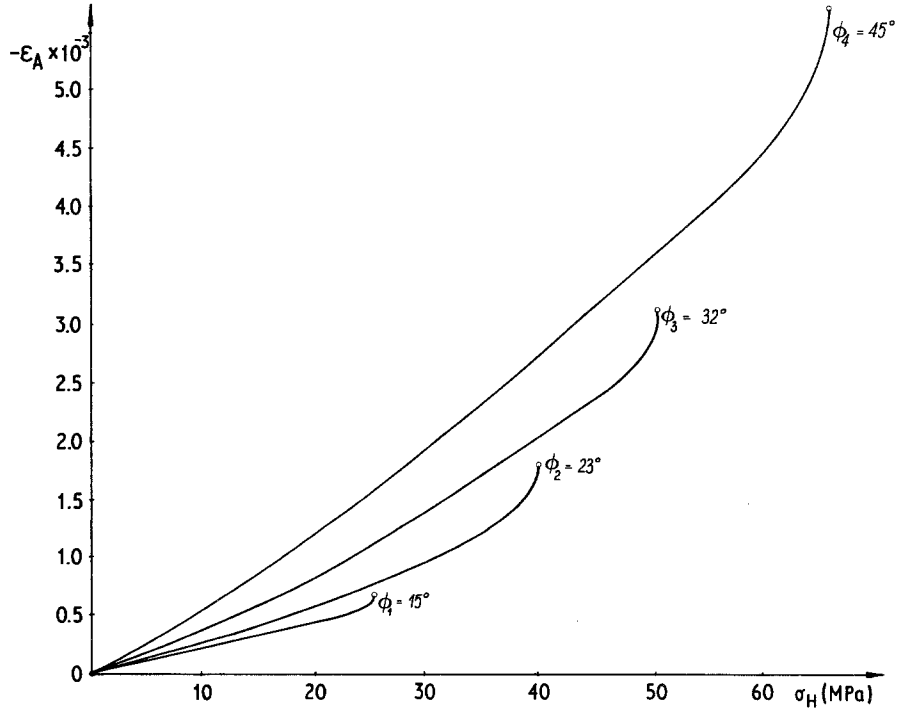

Figure 3 Stress/strain response of pipes with 15°, 23°, 32°, 45°.

TABLE I

Φ	Start of AE			σ_H at the range of non-linearity (MPa)	σ_H fracture (MPa)	N_T at fracture
	σ_H (MPa)	$\sigma_\perp$ (MPa)	$\tau_\parallel$ (MPa)			
15°	13.1	11.1	1.9	> 15	26.0	7×10^4
23°	17.5	11.3	3.8	> 25	41.0	6×10^4
32°	25.1	11.5	6.3	> 35	51.4	4×10^4
45°	28.7	10.9	7.8	> 45	66.6	3×10^4

fibres. The first failure of the composite takes place at the fibre–matrix boundary and is caused mainly by the tensile stress $\sigma_\perp$ (normal to the fibre direction) or the shear stress $\tau_\parallel$ parallel to the fibre. The results of the investigations indicated that for microcracks on the fibre–matrix interface to occur it was necessary to achieve their critical values $\sigma_\perp$ or $\tau_\parallel$.

The state of stress in the lamina under biaxial stress conditions was estimated on the basis of the Puck [10] analysis. In accordance with this theory, the normal stress, $\sigma_\perp$, and the shear stress, $\tau_\parallel$, were determined assuming linear elastic behaviour of the composite material. Golaski *et al.* [4] correlated acoustic emission characteristics as rms voltage and waveform observations to stress state derived from Puck's solution and to various kinds of damage occurring in the pressurized pipes with the same elastic properties and under loading conditions similar to those in the experiment of Hull *et al.* They took into account only the one winding angle of 54°44′, the so-called "ideal angle", receiving a significant start of AE when $\sigma_\perp$ and $\tau_\parallel$ at the matrix–fibre boundary overreached their critical values. The predominance of one stress component responsible for failure during pressure testing was obtained by using two different methods of testing.

In our experiments only the normal stress, $\sigma_\perp$, was predominant through the whole range of the considered winding angles. The variation of the stress ratios $\sigma_\perp/\sigma_H$ and $\tau_\parallel/\sigma_H$ with the winding angles (according to Puck) are shown graphically in Fig. 6.

The dominance of $\sigma_\perp$ over $\tau_\parallel$ is greatest for $\Phi = 15°$ and it decreases with the increase of the winding angle; however, the ratio $\sigma_\perp/\tau_\parallel > 1$ for all Φ. Thus, it can be stated that the initial failure processes which occur in the pipes pressurized under the above loading conditions depends mainly on the tensile stress, $\sigma_\perp$. As a result the separation of the matrix–fibre interfaces or cohesive cracking occurs [8].

An understanding of the fracture mechanisms of the composite material requires a knowledge of the normal stress, $\sigma_\perp$, which acts perpendicularly to the fibre. It was possible to estimate $\sigma_\perp$ by deformation of the hoop-wound pipe made from the same glass and resin under tension (Fig. 7). The failure stress, σ_A^F, under these

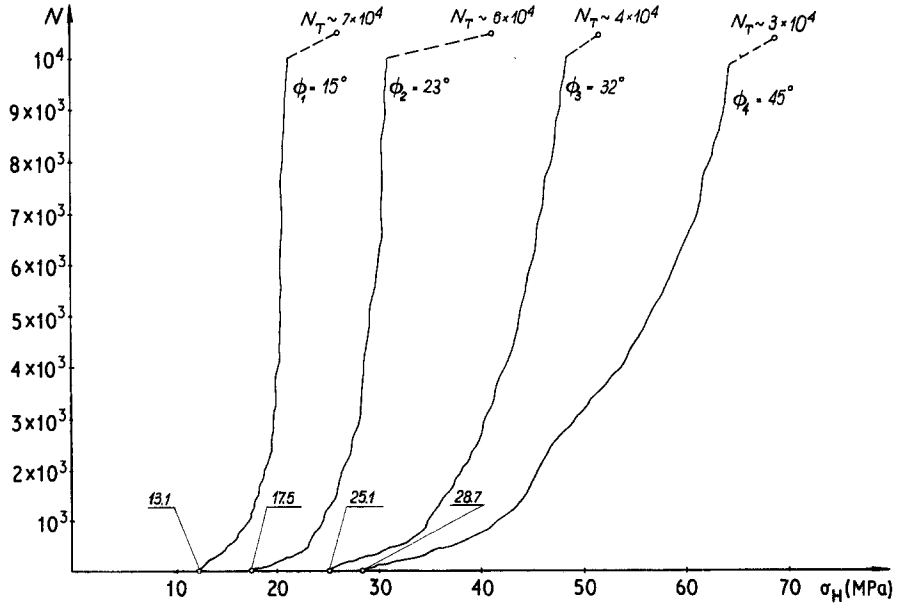

Figure 4 Typical cumulative counts N as a function of σ_H for pipes with 15°, 23°, 32°, 45°.

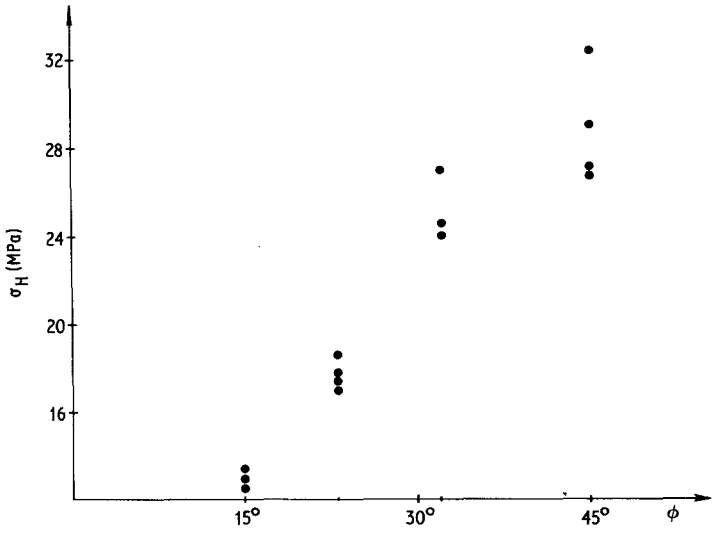

Figure 5 Hoop stress σ_H at the moment of noticeable start of AE as a function of winding angle.

experimental conditions could be attributed to the tensile stress, $\sigma_\perp$, causing debonding at the matrix–fibre boundary, $\sigma_A = \sigma_\perp$ in pipes with arbitrary winding angles. The fracture stress, σ_A^F, of the hoop-wound pipe was at $\sigma_A = 11.5$ MPa and agreed well with the published results [3, 4, 11]. Up to the moment of eventual catastrophic failure by bursting there were no significant AE signals. Strong AE arose just at the moment of fracture when $\sigma_\perp$ overreached its critical value, $\sigma_{\perp c}$, which involved the failure of the pipe at once. Since the critical shear stress, $\tau_{\parallel c}$, is definitely larger than $\sigma_{\perp c}$ [12], it can be assumed the first microcracks were due to $\sigma_\perp$ which exceeded the critical value of 11.5 MPa.

For all the investigated pipes with the four different winding angles the noticeable start of AE was observed at the σ_H of the order of $\sigma_\perp = \sigma_{\perp c}$ (Fig. 5, Table I). AE appeared at the average value of $\sigma_\perp = 11$ MPa. At the moment AE occurred the stresses $\sigma_\perp$ and $\tau_\parallel$ were consistent with a failure criteria in the form of $(\sigma_\perp/\sigma_{\perp A})^2 + (\tau_\parallel/\tau_{\parallel B})^2 = 1$ [9] where $\sigma_{\perp A}$ is the transverse tensile stress in simple uniaxial loading ($\sigma_{\perp A} = \sigma_{\perp C}$) and $\tau_{\parallel B}$ is the fracture stress in shear ($\tau_{\parallel B} = \tau_{\parallel C}$).

In these experiments the ratio $(\tau_\parallel/\tau_{\parallel B})^2$ could be neglected because of its very small value in comparison with $(\sigma_\perp/\sigma_{\perp A})^2$ which was always very close to 1.

The first signs of damage taking place in a pipe were at, or close to, the fibre surface due to debonding of individual fibres (Fig. 8). As the pressure increased, transverse cracks caused by the initial cracks around fibres propagated through the composite (Fig. 9). Transverse

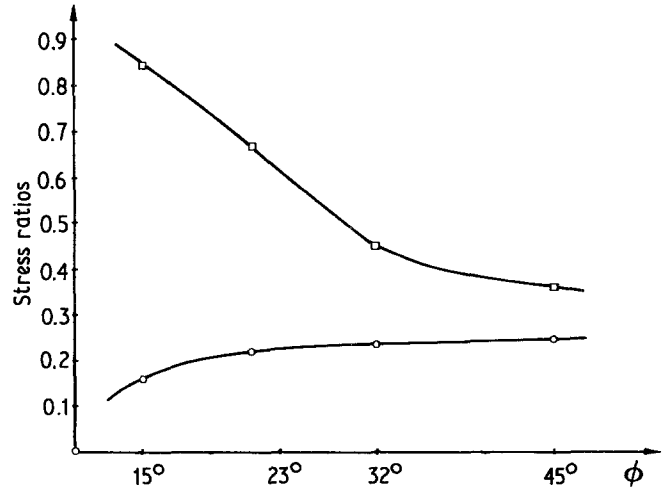

Figure 6 Stress $\sigma_\perp$ and $\tau_\parallel$ related to the fibre direction as a function of winding angle, $V_f = 44\%$. □ – $\sigma_\perp/\sigma_H$, ○ – $\tau_\parallel/\sigma_H$.

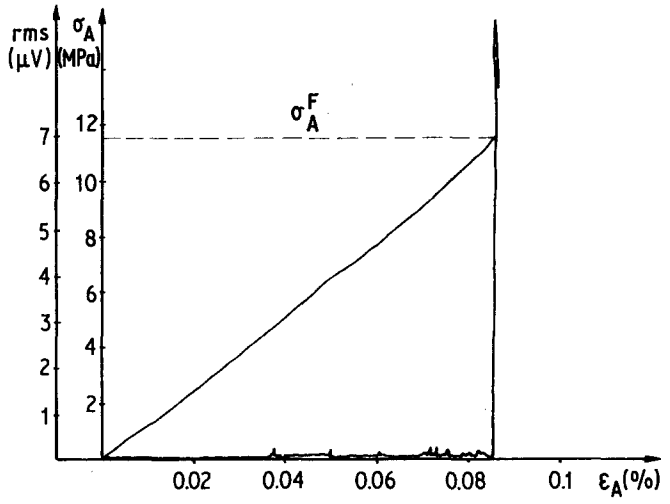

Figure 7 Rms voltage and axial stress σ_A plotted against axial strain for a hoop-wound pipe tested in tension.

cracking was more frequent on the cross-section of the pipe than any type of cracking.

Spencer and Hull [9] correlated the occurrence of whitening of the pipes (as a result of debonding) with the onset of non-linearity at the stresses which were consistent with the failure criterion. The transition to non-linear behaviour of ε_A as a function of σ_H in our experiments was rather broad and it was difficult to estimate exactly the onset of the range of non-linearity of ε_A. It seems that interpretation of the number of counts N, especially the significant start of AE is the most convenient way of establishing the critical state of stress at which the first damage to the composite appears.

Fig. 4 shows that there is some variability in acoustic emission behaviour which occurs between pipes wound at different angles. AE activity decreases with increasing winding angle and the total number of counts N_T is greatest for $\Phi = 15°$. This effect might possibly be caused by friction between fibres or layers of fibres as they slid past each other [4]. The movement of fibres is probably attributable to the stress distribution in the composite material when the principle stress axis lies in a direction similar to that of σ_H and the variation between the principle stress direction and the fibre direction is maximum for $\Phi = 15°$. Hence the generation of AE due to friction is greatest for small winding angles with the high applied stress σ_H.

5. Conclusions

From the above observations, it can be concluded that:

1. acoustic emisison behaviour is strongly dependent on fibre orientations;

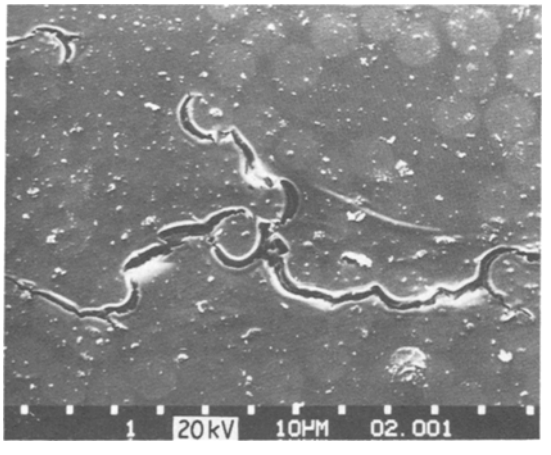

Figure 8 Photomicrograph of cross-section of pipe with $\Phi = 15°$. Initial microcracks at matrix/fibre interface and transverse crack.

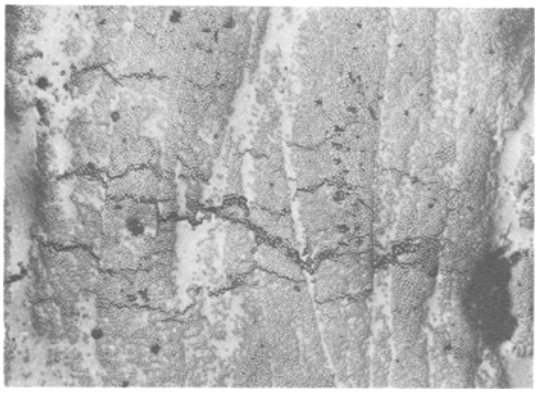

Figure 9 Photo-micrograph of cross-section of pipe with $\Phi = 15°$. Transverse lamina cracks, × 50.

2. with the help of acoustic emission, it is possible to define the critical state of stress at which the first signs of damage of the composite appear;

3. significant occurrence of AE begins as a result of cohesive cracking when the normal stress, $\sigma_{\perp}$, at the matrix–fibre interface overreaches its critical value, $\sigma_{\perp C}$, for all considered fibre winding angles.

Acknowledgement

The authors wish to thank Professor L. Golaski from the University of Wroclaw for valuable discussions and Dr K. E. Evans from the University of Liverpool for his comments on this paper.

References

1. G. D. SIMS, G. D. DEAN, B. E. READ and B. C. WESTERN, *J. Mater. Sci.* **12** (1977) 2329.
2. B. HARRIS, F. J. GUILD and C. R. BROWN, *J. Phys. D. Appl. Phys.* **12** (1979) 1285.
3. M. KUMOSA and L. GOLASKI, in Proceedings of 22nd Meeting of the Acoustic Emission Working Group, Boulder, Colorado, March (1981).
4. L. GOLASKI, M. KUMOSA and D. HULL, *J. Acoustic Emission* **1** (1982) 95.
5. L. GOLASKI, D. HULL, M. KUMOSA, in Proceedings of the Fourth International Conference on Mechanical Behaviour of Materials, Stockholm, August (1983).
6. M. A. HAMSTAD, "Fundamentals of Acoustic Emission", edited by K. Ono (University of California, Los Angeles, 1979) p. 229.
7. D. HULL, M. J. LEGG and B. SPENCER, *Composites* **9** (1978) 17.
8. M. L. C. JONES and D. HULL, *J. Mater. Sci.* **14** (1979) 165.
9. B. SPENCER and D. HULL, *Composites* **9** (1978) 263.
10. A. PUCK, *Kunstoffe* **57** (1967) 284, 573, 965.
11. W. N. BULMANIS and J. I. GUSIEW, *Mech. Kompoz. Mater.* **1** (1983) 47.
12. J. N. RABOTNOW, I. N. DANILOWA, A. P. POLILOW, S. W. SOKOLOWA, I. S. KARPIEIKIN and M. W. WAINBERG, *Mech. Polimer.* **2** (1978) 219.

Received 31 August
and accepted 20 November 1984